# Dimensionality Crossover in Magnetism: From Domain Walls (2D) to Vortices (1D)

A. Masseboeuf,[1,*] O. Fruchart,[2,†] J. C. Toussaint,[2,3] E. Kritsikis,[2,3,4] L. Buda-Prejbeanu,[4] F. Cheynis,[2] P. Bayle-Guillemaud,[1] and A. Marty[5]

[1]*CEA, INAC-SP2M, LEMMA, 17 rue des Martyrs, 38054 Grenoble Cedex 9, France*
[2]*Institut NÉEL, CNRS & Université Joseph Fourier, BP166– F-38042 Grenoble Cedex 9, France*
[3]*Institut National Polytechnique de Grenoble, 38016 Grenoble, France*
[4]*SPINTEC, URA 2512, CEA/CNRS, CEA/Grenoble, 38054 Grenoble Cedex 9, France*
[5]*CEA, INAC-SP2M, NM, 17 rue des Martyrs, 38054 Grenoble Cedex 9, France*

(Received 14 September 2009; revised manuscript received 10 February 2010; published 26 March 2010)

Dimensionality crossover is a classical topic in physics. Surprisingly, it has not been searched in micromagnetism, which deals with objects such as domain walls (2D) and vortices (1D). We predict by simulation a second-order transition between these two objects, with the wall length as the Landau parameter. This was confirmed experimentally based on micron-sized flux-closure dots.

DOI: 10.1103/PhysRevLett.104.127204 PACS numbers: 75.60.Ch

Dimensionality crossover is a rich topic in theoretical and experimental physics. It has been widely addressed in the frame of phase transition and critical exponents, e.g., in magnetism [1,2]. Beyond this microscopic level it is known that materials in an ordered state may be split in domains [3]. In the study of magnetization configurations, a field known as micromagnetism, objects have tentatively been classified according to their dimensionality. Magnetic domains are 3D, domain walls (DWs) are 2D, Bloch lines (i.e., so-called either vortices or antivortices) are 1D, Bloch points are 0D [4,5]. Each class may serve as a boundary to the class of immediately greater dimensionality: DWs are found at domain boundaries, Bloch lines inside domain walls to separate areas with opposite winding [3,5], and Bloch points separate two parts of a vortex with opposite polarities [4,6]. Beyond magnetism, the notions of DWs and vortices are shared by all states of matter ordered with a unidirectional order parameter, i.e., characterized by a vector field $\mathbf{n}$ with $|\mathbf{n}| = 1$. Liquid crystals in the nematic state have a uniaxial order parameter. A strict analogue of magnetic materials is the common case of slabs with anchoring conditions at both surfaces: upon application of a magnetic or electric field perpendicular to the easy axis of anchoring a breaking of symmetry occurs known as the Fredericks transition [7], transforming the order parameter in a unidirectional one. In this case both 180° domain walls and vortices occur [8,9], whose dynamics, topology and annihilation are being studied [10].

The study of magnetic DWs and vortices as objects that can be moved [11] and modified [12–15] in their inner structure is a timely topic, driven by proposals of their use in memory [16] and logic [17] devices. Despite this and the established dimensional classification mentioned above, surprisingly the possibility of a dimensionality crossover between a DW and a vortex has not been addressed. Thus, beyond the aesthetics physical issue of dimensionality crossover, the knowledge of how a DW may switch reversibly to a magnetic vortex should have a great importance in understanding and controlling their static and dynamic features. This transition has not been described either in analogous cases such as liquid crystals.

In this Letter we report on a dimensionality crossover from a DW (2D) to a vortex (1D). Although exemplified in the particular case of magnetic materials, this effect should occur in any state of matter characterized with a unidirectional order parameter. It should be noted that a dimensionality crossover was recently reported for the dynamics of motion of a domain wall along a stripe, whose behavior changes from two-dimensional pinning to one-dimensional pinning on structural defects when the width of the stripe is reduced below typically the distance between major pinning sites [18]. This process however is very different, since it pertains to dynamic processes, and also is extrinsic because it relies on structural defects which depend on the material, method of deposition, and nanofabrication.

For our demonstration we considered epitaxial micron-sized magnetic dots in a flux-closure state. Depending on the dot geometry (size and aspect ratio), the flux may be closed around a vortex [12] or a DW of finite length [19]. The use of an epitaxial material ensures that the results are not biased by microstructural pinning. Besides the dots display sharp and well-defined edges, so that their dimensions can be measured with accuracy. It is known that the topology of Bloch DWs of finite length and of vortices is identical, the former being obtained from the latter by a continuous deformation [19–21]. Thus the question of a transition from a DW to a magnetic vortex arises naturally. We first show by simulation that a wall tends to collapse into a vortex at a critical length of a few tens of nanometers. The transition is of second order, with the wall length as the order parameter. This is confirmed quantitatively by experiments based on micron-sized self-

 

assembled epitaxial dots, both with the dot geometry and an external magnetic field as the driving parameter, showing the generality and robustness of the transition.

Let us describe our methods. Micromagnetic simulations of prisms were performed using GL_FFT, a finite-differences code [22]. The cell size was $3.91 \times 3.91 \times 3.13$ nm or lower and the parameters for bulk Fe were used with an Fe(110) orientation [15]. Simulations of trigonal fcc Co(111) dots were performed using FEELLGOOD, a finite-elements code [23]. The mean cell size was 2.6 nm. Both codes have been custom-developed and are based on the temporal integration of the Landau-Lifshitz-Gilbert equation. The experimental systems consist of self-assembled micron-size Co(111) [24] and Fe(110) [15] dots, epitaxially grown under ultrahigh vacuum using pulsed-laser deposition [25]. These were grown on a single-crystalline 10 nm-thick W buffer layer deposited on sapphire $(11\bar{2}0)$ wafers, and capped with a 5 nm-thick Au layer to prevent oxidation. The wafer was then thinned by mechanical polishing and ion milling. Lorentz microscopy was performed in the Fresnel mode using a JEOL 3010 microscope equipped with a GATAN imaging filter. In this mode DWs (vortices) are highlighted as dark or bright lines ( dots) depending on the chirality of magnetization curling around the DW or vortex [26]. The images are formed with a dedicated mini-lens, while an axial magnetic field can be added using the conventional objective lens.

We first present the results of simulation. As a textbook case we consider flat prismatic dots with fixed height-over-width ratio 0.2 and thickness 50 nm and above. The prismatic shape and use of finite differences ensure high accuracy results for the description of the phase transition. The length, taken along the in-plane Fe[001] direction, is varied from 1 to 1.5 with respect to the width. As expected for elongated dots of such thickness [19–21] a Landau state occurs, displaying two main longitudinal domains separated by a Bloch DW [Figs. 1(b) and 1(d)]. The DW displays perpendicular magnetization in its core, while it is terminated at each surface by an area with in-plane magnetization, the *Néel* caps [27]. At each end of the DW the magnetic flux escapes through a surface vortex. We define the length of the DW as the distance between the projections into the film plane of the locii of these two vortices [Fig. 1(d)]. From this definition a vortex is a DW with zero length, such as found, e.g., for a dot with a square base [Figs. 1(a) and 1(c)]. Series of simulations of the equilibrium state for variable dot length were performed. At each stage the magnetization map is stretched or compressed along the length to serve as a crude input for the map of the next value of length, for which the equilibrium state is again calculated. The series was performed once with rising length, then again with decreasing length back to the square base. This yielded identical results, ruling out the possibility of metastable configurations biasing the results. To avoid discretization artifacts the number of cells

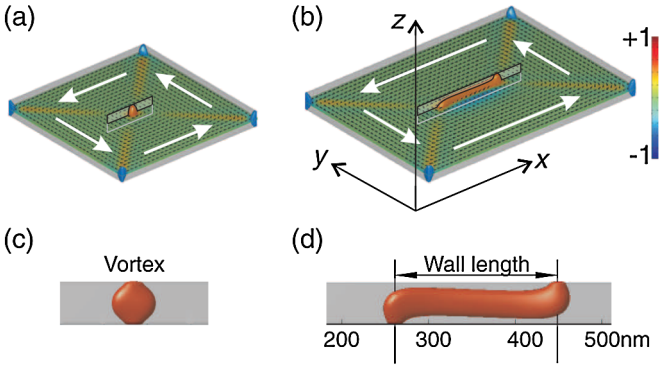


FIG. 1 (color online). Simulated magnetization states in flat Fe(110) dots with size (a) $500 \times 500 \times 50$ nm: vortex state and (b) $500 \times 750 \times 50$ nm: Landau state consisting of a Bloch wall separating two antiparallel domains. The color stands for the direction of magnetization along $z$, see right scale. In these open views the only parts displayed as volumes are those were $m_z$ is greater than 0.5. This highlights the central vortex or Bloch wall (red) and the magnetization areas close to the vertical edges of the prisms (blue). At all other places the surface displays magnetization in the midheight plane. (c)–(d) Views in the $xz$ plane, corresponding to the framed areas in (a)–(b), respectively.

was kept constant for all simulations of a dot of given height. Instead, the length of each cell was varied progressively to fit the dot length. The dependence of the DW length with the dot length is shown on Fig. 2(a). For largely elongated dots the wall length increases linearly with slope 1. In this regime the two surface vortices are sufficiently apart one from another to have a negligible interaction. Their position is essentially determined by the minimization of the energy of the triangular closure domain along the two short sides of the dot. On the reverse in the low-length regime the DW length decreases faster than slope 1, so that the vortex state is reached before the dot has a square base. We define the *collapsed* length as the difference between the length of dot upon the collapse and the asymptotic linear variation of wall length for an elongated dot [Fig. 2(a)]. Plotting the square of the DW length versus the dot length reveals a linear variation. The crossover is therefore Landau-like, i.e., of second order. Such transitions are associated with a breaking of symmetry, which in the present case is whether the top surface vortex shifts towards $+x$ or $-x$. The results are qualitatively similar for other thicknesses. Figure 2(b) shows the results of similar finite-element simulations applied to trigonal Co(111) dots also 50 nm-thick, which display the very same physics. This suggests that the crossover is a general phenomenon, independent from the exact shape of the system.

These predictions have been confirmed experimentally. We first consider self-assembled face-centered cubic Co(111) dots. These have a trigonal symmetry reflecting their crystalline structure, with a base close to a regular hexagon [Fig. 3(b)] [24]. Whereas previous studies on such systems were dealing with very thin dots thus found in a

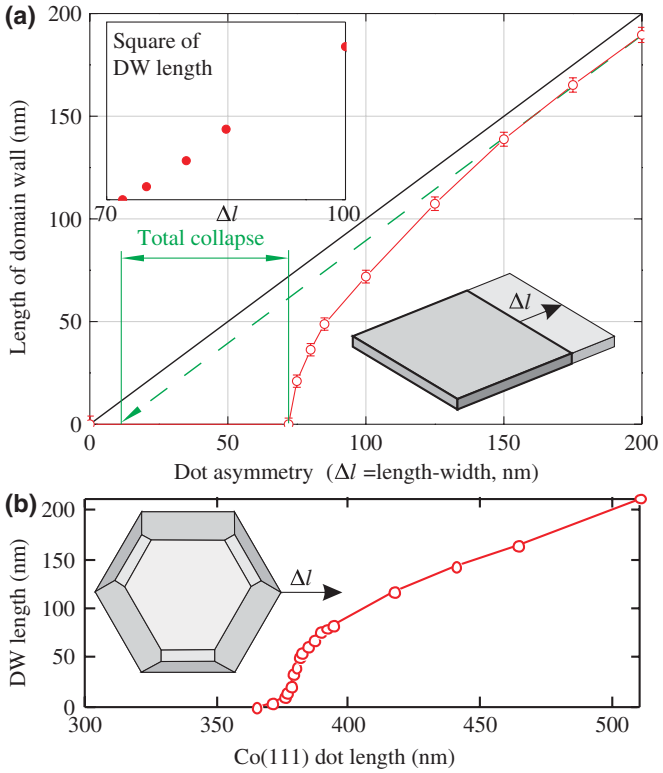


FIG. 2 (color online). (a) Open symbols: length of the Bloch wall in the simulated Landau state in an Fe(110) dot of thickness 50 nm, plotted versus the dot lateral asymmetry $\Delta l$ (length minus width, see inset sketch). Linear line with slope +1: wall length in the simple geometrical van den Berg model (black line). Dotted line: asymptotic extrapolation from long dot, whose intercept with the $x$ axis defines the total collapsed. Inset: squared length of Bloch wall, same $x$ axis. (b) Similar simulations based on a Co(111) dot, here 50 nm-thick. The inset shows the detailed faceted shape of these dots [24].

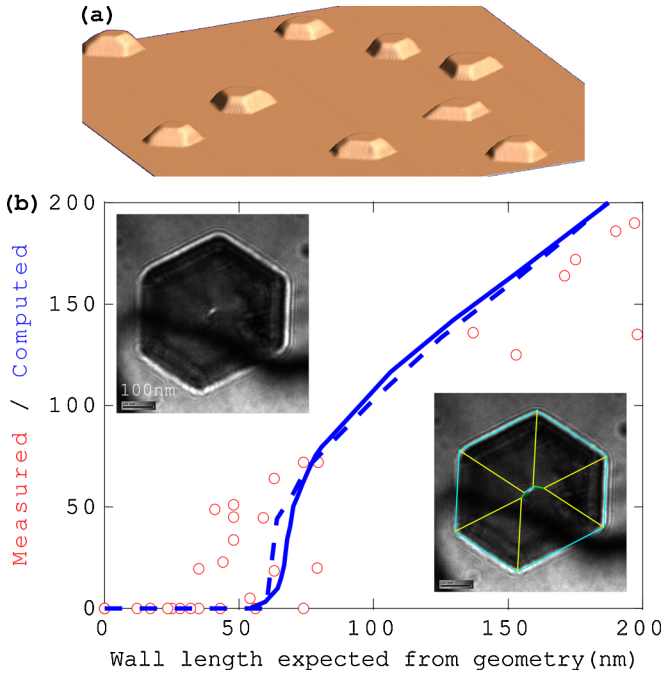


FIG. 3 (color online). (a) True $Z$-scale 3D view of a $6 \times 6$ $\mu$m AFM image of self-assembled Co(111) dots (b) Open symbols: DW length measured in Co(111) dots plotted versus the length expected from the geometrical van den Berg construction. The predictions from simulations for the estimated thickness of the dot 116 nm are superimposed without adjustment, as guide to the eye, both for Fe(110) (dotted line) and Co(111) (full line). Insets: typical Co dot displaying a vortex (upper left) along with the associated construction predicting a DW (lower right, central blue line).

nearly single-domain state [28], the thickness of our dots is in the range 50–200 nm inducing flux-closure states around a DW or vortex. These dots are perfectly suited for our needs because owing to the natural spread of shape occurring in self-assembly we can study the length of DWs as a function of the dot aspect ratio, by a statistical investigation of an assembly of dots over the same sample. For each dot we measured the experimental DW length, and computed the expected DW length predicted by the simple van den Berg geometrical construction. This construction is relevant for vanishing thickness and infinite dimensions [29], and equals the dot asymmetry used in the simulations so that a direct comparison with the data of Fig. 2 is possible. Figure 3(b) summarizes this analysis, performed over more than 30 dots. The collected results are quantitatively consistent with the simulation predictions. The experimental spread of points may be attributed first to errors in the measurement of both the DW length and dot dimensions, second to the spread of dot thickness as the collapsing length slightly depends on the thickness. Despite this spread, it shall be noticed that only vortices are observed when the expected length lies below 40 nm. This cannot be attributed to an experimental limitation to identify short DWs, as many DWs with length below 40 nm have been measured. These however all lie for expected wall length above 40 nm. These correlations lie above statistical fluctuations, which unambiguously demonstrates the collapse of DWs towards vortices in a quantitative agreement with simulations.

To demonstrate the generality and robustness of the vortex-DW transformation we now consider an external field as the driving parameter for the transition. In this case we use Fe(110) dots, which by their crystallographic nature are elongated [25] [Fig. 4(a)]. Upon applying the saturating field with a tilt angle of a few degrees with respect to the normal to the plane, and the in-plane component oriented along its short length, the dot can be prepared in a diamond state, i.e., consisting of two flux-closure parts with opposite chiralities [Fig. 4(b)]. It happens that the application of a tilted field of moderate magnitude affects the length of the DWs [Fig. 4(c)] in a continuous way. The length of the DW to the right of the dot decreases with increasing field. When its reaches $21 \pm 3$ nm, which is comparable to the collapse length mentioned above, a stochastic switching was observed in real time between a Bloch wall and a vortex state

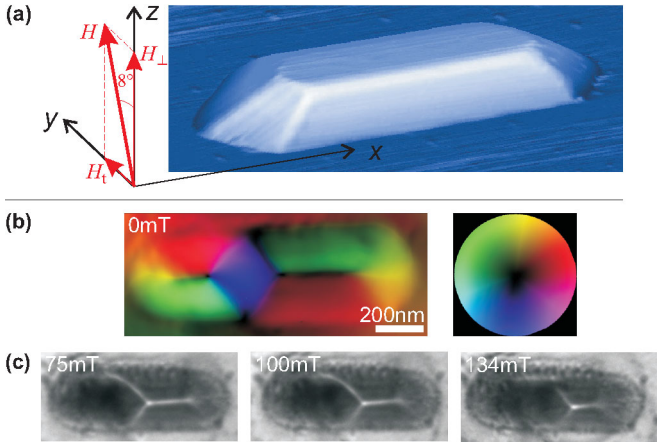


FIG. 4 (color online). (a) True $Z$-scale 3D AFM view of a typical Fe(110) dots, along with the geometry of the applied field. (b) map of the in-plane magnetization of a similar dot found in the diamond state, reconstructed from Fresnel images taken at different defocusing. (c) Series of Fresnel images of the same dot taken under a magnetic field applied tilted towards $y$. The labels indicate the value of the $y$ component of the field.

with a characteristic time constant of 100 ms (see supplementary material). This confirms that the top and bottom surface vortices undergo a short-range attractive force, which is the driving force for the transition.

To conclude, we addressed the dimensionality crossover of a magnetic domain wall (DW, 2D) into a magnetic vortex (1D). Simulations and experiments agree quantitatively that DWs collapse into vortices at a critical length of a few tens of nanometers, which reveals a short-ranged attractive force between the two ends of a DW. Beyond physics aesthetics, our investigation should prove useful when analyzing the increasing number of experiments dealing with the behavior of domain walls and vortices under the effect of pulsed magnetic fields or spin-polarized currents, which undergo complex variations of shape and length during their dynamics. This includes the case of, e.g., the vortex state, where a domain wall dynamically replaces the vortex [30], or the multiplication of vortices or transformation of the type of domain wall in magnetic stripes [31,32].

*Present address: CEMES, 29 rue Jeanne Marvig, BP 94347, 31055 Toulouse Cedex 4, France.
†Corresponding author.
Olivier.Fruchart@grenoble.cnrs.fr

[1] N. D. Mermin and H. Wagner, Phys. Rev. Lett. **17**, 1133 (1966).
[2] P. Poulopoulos and K. Baberschke, J. Phys. Condens. Matter **11**, 9495 (1999).
[3] A. Hubert and R. Schäfer, *Magnetic Domains. The Analysis of Magnetic Microstructures* (Springer, Berlin, 1999).
[4] W. Döring, J. Appl. Phys. **39**, 1006 (1968).
[5] A. S. Arrott and T. L. Templeton, Physica (Amsterdam) **233B**, 259 (1997).
[6] A. Thiaville, J. M. García, R. Dittrich, J. Miltat, and T. Schrefl, Phys. Rev. B **67**, 094410 (2003).
[7] H. Zocher, Faraday Soc. **29**, 945 (1933).
[8] F. Brochard, J. Phys. **33**, 607 (1972).
[9] P. G. de Gennes, *The Physics of Liquid Crystals* Int. Series Monographs 83 (Oxford Science Publications, Oxford, 1974).
[10] C. Blanc, D. Svensek, S. Zumer, and M. Nobili, Phys. Rev. Lett. **95**, 097802 (2005).
[11] J. Grollier, P. Boulenc, V. Cros, A. Hamzic, A. Vaurès, A. Fert, and G. Faini, Appl. Phys. Lett. **83**, 509 (2003).
[12] T. Okuno, K. Shigeto, T. Ono, K. Mibu, and T. Shinjo, J. Magn. Magn. Mater. **240**, 1 (2002).
[13] B. Van Waeyenberge, A. Puzic, H. Stoll, K. W. Chou, T. Tyliszczak, R. Hertel, M. Fähnle, H. Brückl, K. Rott, G. Reiss, I. Neudecker, D. Weiss, C. H. Back, and G. Schütz, Nature (London) **444**, 461 (2006).
[14] R. Hertel, S. Gliga, M. Fähnle, and C. M. Schneider, Phys. Rev. Lett. **98**, 117201 (2007).
[15] F. Cheynis, A. Masseboeuf, O. Fruchart, N. Rougemaille, J. C. Toussaint, R. Belkhou, P. Bayle-Guillemaud, and A. Marty, Phys. Rev. Lett. **102**, 107201 (2009).
[16] J.-G. Zhu, Y. Zheng, and G. A. Prinz, J. Appl. Phys. **87**, 6668 (2000).
[17] D. A. Allwood, G. Xiong, C. C. Faulkner, D. Atkinson, D. Petit, and R. P. Cowburn, Science **309**, 1688 (2005).
[18] K.-J. Kim, J.-C. Lee, S.-M. Ahn, K.-S. Lee, C.-W. Lee, Y. J. Cho, S. Seo, K.-H. Shin, S.-B. Choe, and H.-W. Lee, Nature (London) **458**, 740 (2009).
[19] P. O. Jubert, J. C. Toussaint, O. Fruchart, C. Meyer, and Y. Samson, Europhys. Lett. **63**, 132 (2003).
[20] A. S. Arrott, B. Heinrich, and A. Aharoni, IEEE Trans. Magn. **15**, 1228 (1979).
[21] R. Hertel and H. Kronmüller, Phys. Rev. B **60**, 7366 (1999).
[22] J. C. Toussaint, A. Marty, N. Vukadinovic, J. Ben Youssef, and M. Labrune, Comput. Mater. Sci. **24**, 175 (2002).
[23] E. Kritsikis, J. C. Toussaint, O. Fruchart, and L. D. Buda-Prejbeanu (to be published).
[24] O. Fruchart *et al.* (unpublished).
[25] O. Fruchart, M. Eleoui, P. O. Jubert, P. David, V. Santonacci, F. Cheynis, B. Borca, M. Hasegawa, and C. Meyer, J. Phys. Condens. Matter **19**, 053001 (2007).
[26] J. N. Chapman, J. Phys. D **17**, 623 (1984).
[27] A. Hubert, Phys. Status Solidi **32**, 519 (1969).
[28] D. Li, C. Yu, J. Pearson, and S. D. Bader, Phys. Rev. B **66**, 020404(R) (2002).
[29] H. A. M. van den Berg, J. Magn. Magn. Mater. **44**, 207 (1984).
[30] D. H. Kim, B. L. Mesler, E. Anderson, P. Fischer, J.-H. Moon, and K. J. Lee (2010) under review.
[31] Y. Nakatani, A. Thiaville, and J. Miltat, Nature Mater. **2**, 521 (2003).
[32] M. Kläui, M. Laufenberg, L. Heyne, D. Backes, U. Rüdiger, C. A. F. Vaz, J. A. C. Bland, L. J. Heyderman, S. Cherifi, A. Locatelli, T. O. Mentes, and L. Aba, Appl. Phys. Lett. **88**, 232507 (2006).